

Deformation and failure characteristics of rectangular clay specimens under three-dimensional condition

Déformations et fissures caractéristiques d'un échantillon d'argile rectangulaire sous condition tridimensionnelle

T. KODAKA, Y. HIGO & T. TAKYU, Department of Civil Engineering, Kyoto University, Kyoto, Japan

ABSTRACT: In order to grasp deformation and failure behaviors of clay under 3-D condition as well as large deformation and strain localization, a series of triaxial compression tests using rectangular clay specimens with different heights and width are conducted. To use the rectangular specimen is convenient for this object. Shear strain distribution localized with compression is also successfully observed by taking digital photograph from two side of rectangular specimens and image analysis of their digital photograph. It is found that the bifurcation phenomena, e.g. formation and progress of various shear planes, failure with buckling, existence of a bifurcation point and following instability on load – displacement curves, can be clearly observed in the present tests.

RÉSUMÉ: Afin de comprendre le comportement de la déformation et de la rupture de l'argile sous conditions tridimensionnelles dans le cas des grands déplacements et de la localisation des déformations, de nombreux essais de compression triaxiale sur des échantillons rectangulaires d'argile avec différentes hauteurs et profondeurs ont été conduits. L'utilisation d'échantillon rectangulaire est très pratique pour cette recherche. La distribution des déformations de cisaillement localisées par la compression a été observée avec succès en analysant les photographies numériques prises de 2 cotés de l'échantillon rectangulaire. Il a été trouvé que le phénomène de bifurcation, c'est à dire la formation et la progression de différents plans de cisaillement, la rupture avec flambement, l'existence d'un point de bifurcation et l'instabilité des courbes chargement-déplacement qui en résultent, peut être clairement observé dans les présents tests.

1 INTRODUCTION

Clarification and predictions of strain localization of geomaterials are indispensable research topics to improve an accuracy of computation of the geotechnical engineering problems. Most of past numerical studies concerning the strain localization have been done under the plane strain conditions (e.g. Yatomi et al. 1989, Oka et al. 1994, Asaoka and Noda 1995, Oka et al. 1996, Asaoka et al. 1997a, Asaoka et al. 1997b, Oka et al. 1997, Oka et al. 2001) and most of experimental researches are done by the triaxial tests using cylindrical specimen (e.g. Ikeda and Goto 1993, Asaoka et al. 1997a, Asaoka et al. 1997b) or by the plane strain tests (Yoshida et al. 1994, Yoshida and Tatsuoka 1997). Nowadays, three-dimensional numerical analysis becomes actual computational tool not only for research works but also for design works. With respect to the strain localization in the ground, large difference between two- and three-dimensional analyses exists. It is necessary to analyze ground under three-dimensional condition to consider the shear band formation. In the present study, in order to grasp the deformation and failure behaviors of geomaterials as true three-dimensional phenomena, the triaxial compression test using the rectangular clay specimen was conducted. By using the rectangular specimen, it is easy to set up the boundary conditions in the three-dimensional computation work. In addition, since a transverse section of specimen does not have many axis of symmetry compared with the cylindrical specimen,

it is relatively easy to observe the strain localization. The distribution of shear strain observed in side of specimen can be obtained by the image analysis of digital photographs.

2 TEST PROGRAM

The physical properties of clay sample are listed in Table 1. Normally consolidated clay sample that was prepared by remolding and then pre-consolidation was trimmed to be rectangular shape. The shapes of specimens in each case are illustrated in Table 2 and Fig. 1. The specimens were isotropically consolidated to 196 kPa (cell pressure 392 kPa and back pressure 196 kPa), and then subjected to a standard undrained compression test. The stress – strain relationship of soil specimen was measured by load cell and LVDT. To obtain local shear strain distributions observed in a side of specimen, a digital camera took the photographs of side surface of specimen, which were drawn 5mm meshes, and then the image analysis in the digital photographs was done. Fig. 2 shows an example of taken digital photographs.

Table 1. Physical properties of clay sample.

G_s (g/cm ³)	w_L (%)	w_p (%)	I_p	Sand (%)	Silt (%)	Clay (%)
2.64	59.1	27.4	31.7	9.8	56.2	34.0

Table 2. Test cases.

CASE	Scale of transverse section $W_1 \times W_2$ (cm)	Height H (cm)	H/W ratio	Loading rate (%/min)
	4 × 4	12	3	1.0, 0.1, 0.01
	4 × 4	8	2	0.1
	4 × 2	8	4	0.1
	4 × 4	4	1	0.1
	φ5 (cylinder)	10	2	0.1

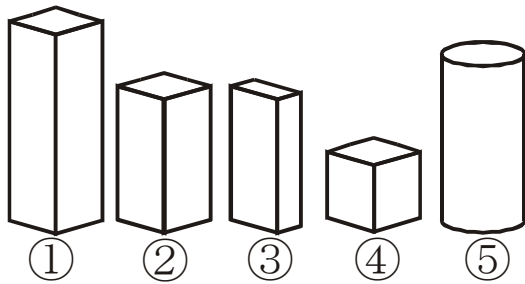


Figure 1. Shapes of specimens

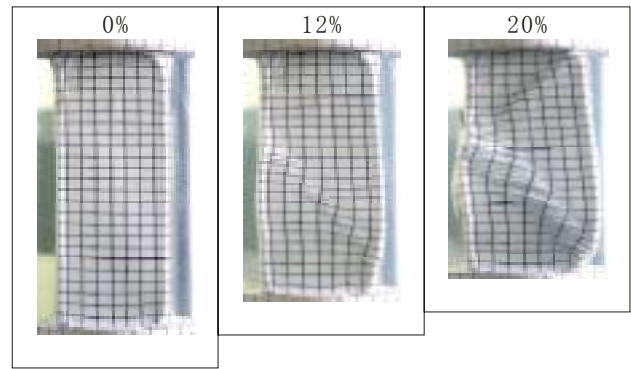


Figure 2. Deformation of specimen (CASE -3)

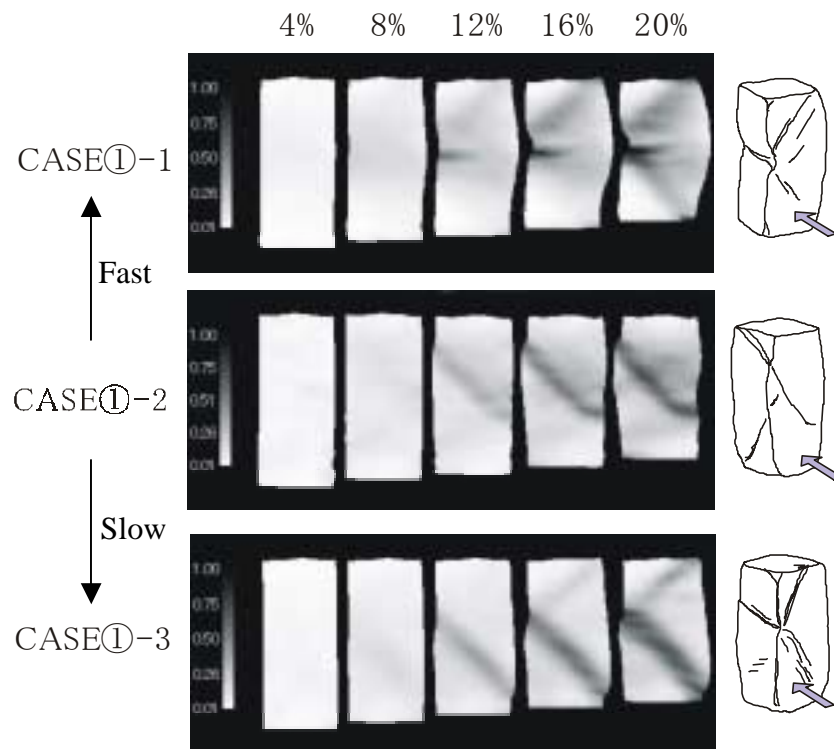


Figure 3. Shear strain distributions in CASE

3 TEST RESULTS

3.1 Effect of loading rate

Three axial strain rate was used only in CASE 1 to investigate the effect of loading rate on failure mechanism of rectangular clay specimen. The local shear strain distributions obtained by the image analysis in digital photograph with different axial strain levels are shown in Fig. 3. Shear planes were clearly observed in any specimens and the local shear strain exceeds 100% near the shear plane. The sketches of specimens after testing as well as shear planes are shown in Fig. 4. In the case of middle and slow loading rate, i.e. CASE 1-2 and 1-3, two shear planes cut through the specimen crossing each other. It is, however, observed the different type failure pattern in the fastest loading case, CASE 1-1, which likes the buckling of column. Fig. 5 shows the relationships between a deviator stress and an axial strain, which were obtained using same shape specimens; CASE 1-1 (4 × 4 × 12cm). In the initial part of stress - strain curve, the

fastest case, i.e. CASE 1-1, shows largest deviator stress among three cases. This tendency agrees with a traditional theory of time effect of clay. After peak strength, however, the deviator stress of CASE 1-1 rapidly decreases to be the smallest residual strength. The decrease of deviator stress of CASE 1-1 is more significant than the other cases. It seems to be due to the buckling failure pattern of the fastest loading case. Asaoka and Noda (1995) and Asaoka et al. (1997a) showed the following results by the triaxial compression tests and the numerical experiments of remolded normally consolidation clay. "Higher order bifurcation mode can be observed in the faster loading test cases, in which the deviator stress shows larger. In the slowest loading case, only 1st order bifurcation mode can be finally observed going through the mode switching, in which the deviator stress shows relatively small." The buckling failure pattern observed by the present test seems to be similar to 2nd order bifurcation mode mentioned by Asaoka and Noda (1995). However, the peak and residual strength of this failure pattern are not larger than that of shear failure pattern like 1st bifurcation mode.

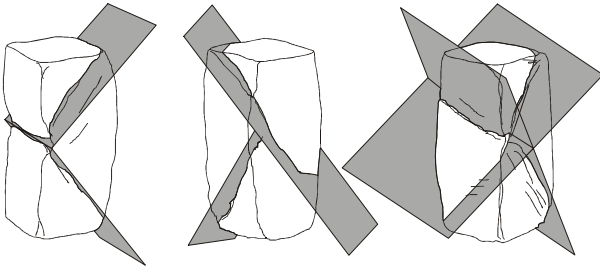


Figure 4. Patterns of shear plane formation

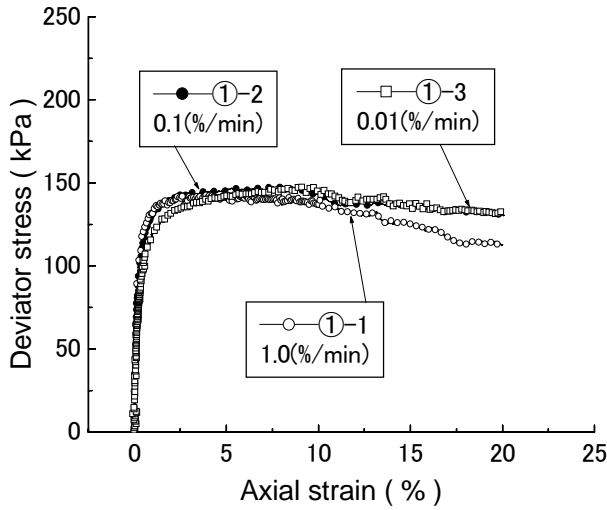


Figure 5. Stress – strain curves in CASE

3.2 Effect of slenderness of specimens

Fig. 6 shows the stress – strain relationship and local shear stress distributions with different axial strain in CASE . Since the slenderness ratio is smaller than CASE , unstable behavior shown in Fig. 5 cannot be seen in this case, and the stress – strain relationship is very stable even in a large axial strain level. It is observed two shear bands on a side surface of specimen as X character. This type of failure pattern can be considered higher order bifurcation mode compared with the single significant shear band failure pattern observed in CASE -2 and -3 (Ikeda and Murota 1997). Fig. 7 shows the stress – strain relationship and deformed specimen due to compression in CASE , which is observed the clear buckling pattern on the narrow side surface, i.e. 8cm height \times 2cm width (H/W ratio: 4). It is easy to understand that the deviator stress is unstable after peak strength and directly refracts the deformation of specimen. The relationships between deviator stress and axial strain are shown in Fig. 8 together with all cases. In all cases, changes of the stress-strain curves are related to the shear plane formation and progress. When the shear plane is observed, the deviator stress decreases. Fig. 9 shows the load - displacement relationships, which are rearranged instead of Fig.8. Deviator stresses in Fig.9 are just axial loads divided by their initial sectional areas. It can be seen that the load-displacement curves in the initial loading stage are almost unique curve in all cases, and then they diverge from a bifurcation point. After the bifurcation, the specimen that has larger H/W ratio presents more unstable behavior.

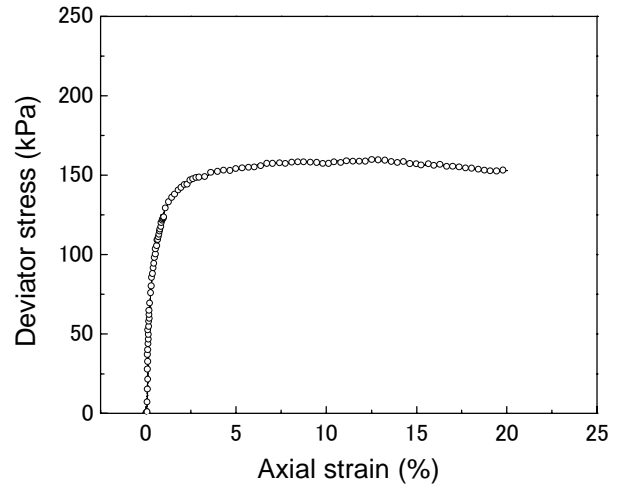


Figure 6. Stress – strain relationship and shear strain distributions in CASE

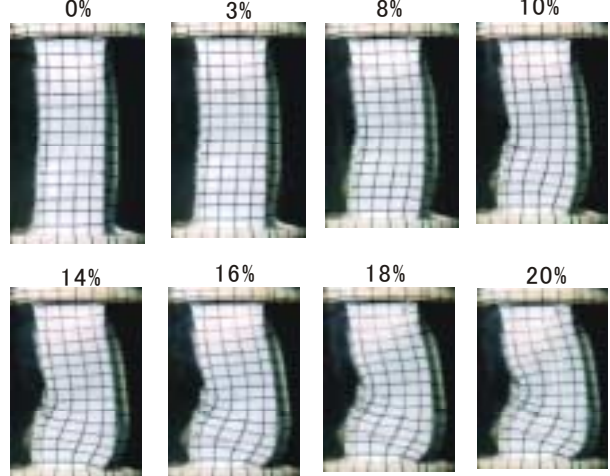
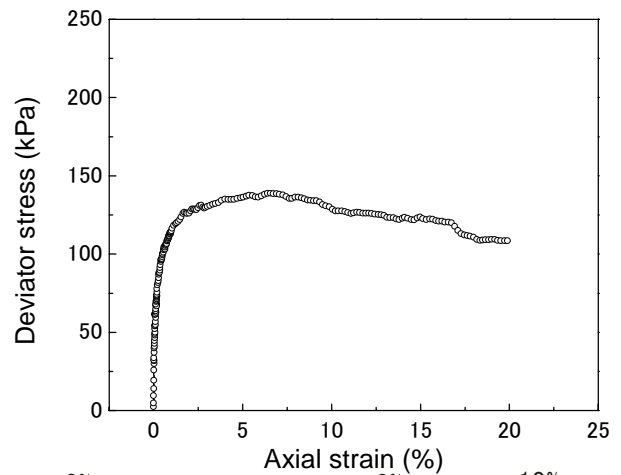


Figure 7. Stress – strain relationship and deformed specimen in CASE

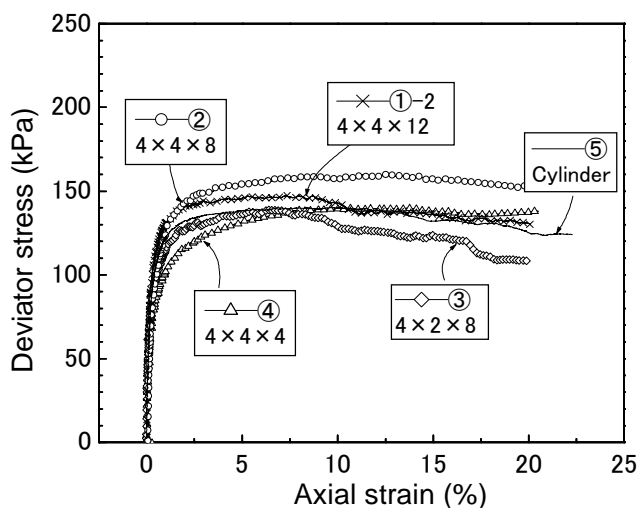


Figure 8. Stress – strain curves

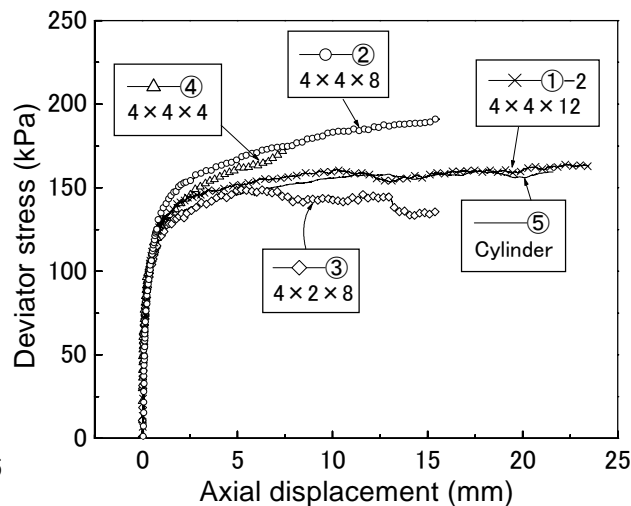


Figure 9. Load – displacement curves

4 CONCLUSIONS

In the present study, triaxial compression tests using rectangular clay specimen with different height and sectional shapes are conducted to discuss the three-dimensional failure behavior of clay. The local shear strain distributions are measured by the image analysis in digital photograph taken in side surfaces of specimen during the triaxial compression test. The results obtained are as follows.

- 1) Shear planes were clearly observed in any specimens and the local shear strain exceeds 100% near the shear plane.
- 2) The shear failure pattern and buckling failure pattern were observed in the slow and fast loading rate test, respectively.
- 3) Even though the similar shear failure pattern is observed, the different bifurcation mode, i.e. formation pattern and number of shear band, occurs depending on the slenderness ratio.
- 4) It seems to exist a bifurcation point. After passing this point, unstable behavior on load – displacement curves can be clearly observed.

Discussion of large deformation and failure behavior using the slender specimens cannot directly link to the practical problems. It is, however, very important that the minute observation of the typical strain localizations in the specimen to improve the accuracy of prediction of progressive failure in numerical computation.

ACKNOWLEDGEMENTS

The authors wish to acknowledge the useful suggestions and kindly support of Prof. F. Oka of Kyoto University.

REFERENCES

- Asaoka, A. & Noda, T. 1995. Imperfection-sensitive bifurcation of Cam-clay under plane strain compression with undrained boundaries. *Soil and Foundations* 35(1): 83-100.
- Asaoka, A., Nakano, M., Noda, T. & Kaneda, K. 1997a. Undrained creep rupture of normally consolidated clay triggered by the “mode switching” during pore water migration. In A. Asaoka, T. Adachi & F. Oka (eds), *Deformation and Progressive Failure in Geomechanics; Proc. Intern. Symp., Nagoya, 1997*: 21- 26. Pergamon.
- Asaoka, A., Nakano, M., Noda, T., Takaine, T & Kaneda, K. 1997b. Progressive failure of heavily overconsolidated clay under constant load application, an experiment and its simulation. In A. Asaoka, T. Adachi & F. Oka (eds), *Deformation and Progressive Failure in Geomechanics; Proc. Intern. Symp., Nagoya, 1997*: 69 - 74. Pergamon.
- Ikeda, K & Goto, S. 1993. Imperfection sensitivity for size effect of granular materials. *Soils and Foundations* 33(2): 157 - 170.
- Ikeda, K. & Murota, K. 1997. Recursive bifurcation as sources of complexity in soil shearing behavior, *Soils and Foundations*. 37(3): 17 - 29.
- Oka, F, Adachi, T. & Yashima, A. 1994. Instability of an elasto-viscoplastic constitutive model for clay and strain localization. *Mechanics and Materials* 18: 119 - 129.
- Oka, F, Adachi, T. & Yashima, A. 1996. A strain localization analysis using a viscoplastic softening model for clay. *Intern. Jour. Plasticity* 11(5): 523 - 545.
- Oka, F, Yashima, A., Sawada, K & Adachi, T. 1997. Effect of viscoplastic strain gradient on strain localization analysis. In A. Asaoka, T. Adachi & F. Oka (eds), *Deformation and Progressive Failure in Geomechanics; Proc. Intern. Symp., Nagoya, 1997*: 27 - 32. Pergamon.
- Oka, F., Jiang, M. & Higo, Y. 2001. Gradient dependent viscoplastic constitutive models and strain localization analysis of water saturated cohesive soil. In Desai et al. (eds.). *Computer Methods and Advances in Geomechanics, Proc. Intern. Symp. Tuson. 2001*: 519 - 524.
- Yatomi, C., Yashima, A., Iizuka, A. & Sano, I. 1989. General theory of shear band formation by a non-coaxial CAM-CLAY model. *Soils and Foundations* 29(3): 41 - 53.
- Yoshida, T., Tatsuoka, F., Siddiquee, M.S.A., Kamegai, Y. & Park, C.-S. 1994. Shear banding in sand in plane strain compression. In Chambon et al. (eds.). *Proc 3rd Intern. Workshop on Localization and Bifurcation Theory for Soils and Rocks, Grenoble, 1994*: 165 - 179.
- Yoshida, T. & Tatsuoka, F. 1997. Deformation properties of shear band subjected to plane strain compression and its relation to particle characteristics. *Proc. 14th ICSMGE, Hamburg 1*: 237 - 240.